JOURNAL OF SOLID STATE CHEMISTRY 117, 88–96 (1995)

Determination of Layer Structure in $Sr_{1-x}La_xTiO_{3+0.5x}$ ($0 < x < 1$) Compounds by High-Resolution Electron Microscopy

M. E. Bowden, D. A. Jefferson, and I. W. M. Brown*

*Department of Chemistry, University of Cambridge, Cambridge CB4 1BY United Kingdom; and *New Zealand Institute for Industrial Research and Development, P.O. Box 31-310, Lower Hutt, New Zealand*

Received June 8, 1993; accepted July 23, 1993

High resolution electron microscopy has shown that samples of La-substituted $SrTiO_3$ prepared in oxidizing atmospheres contain oxygen-rich layers parallel to a perovskite {110} plane. These layers have the same structure as those found in $La_2Ti_2O_7$ and explain how the excess oxygen required by the altervalent substitution is incorporated into the structure. At low levels of substitution, layers occurred predominantly in clusters irregularly distributed within the host perovskite. Increasing substitution, and therefore increasing frequency of the layers, led to new ordered compounds corresponding to the $n = 4.5$ and $n = 5$ members of the compositional series $Sr_{n-4}La_4Ti_nO_{3n+2}$. © 1995 Academic Press, Inc.

INTRODUCTION

$SrTiO_3$ is an example of a perovskite compound which exhibits ideal cubic symmetry. Many workers have examined ionic substitutions in this material in order to study the effects on its electronic properties. Reports of La^{3+} substitution for Sr^{2+} are intriguing because, when it is performed in oxidizing atmospheres, charge neutrality dictates that the resultant compound should contain additional oxygen beyond the perovskite ABO_3 composition (i.e., $Sr_{1-x}La_xTiO_{3+0.5x}$). The question then arises as to how this extra oxygen is accommodated into the structure.

Initial preparations (1) of a composition corresponding to $x = 0.2$ yielded a two-phase mixture of $SrTiO_3$ and La_2O_3 and so it was thought that only limited solubility of La in $SrTiO_3$ was possible. However, subsequent publications (2, 3) reported a more extensive solid solution, in (3) of up to 40 at.% La in which X-ray diffraction detected only a single perovskite phase. Eror and Balachandran (4) also measured the reversible weight change which occurred when these samples were heated in alternately reducing and oxidizing atmospheres. They found that the charge imbalance produced by substituting La^{3+} for Sr^{2+} was compensated for by the partial reduction of Ti^{4+} to Ti^{3+} in reducing atmospheres, and by the incorporation of additional oxygen into the structure in oxidizing atmospheres. Because of the relatively large concentrations involved it was considered unlikely that the extra oxygen could be present at the grain boundaries, in an additional phase, or in interstitial lattice sites. Instead it was thought that planes of SrO with the same structure as that found in the series of layered compounds $Sr_{n+1}Ti_nO_{3n+1}$ (5, 6) formed within the perovskite matrix. Tilley (7) has shown that such planes do not form an ordered array at the frequency expected for this composition, and this may explain why X-ray diffraction patterns do not appear to show a new phase. In order to maintain the correct cation stoichiometry, the model (4) also proposed that some of the Sr sites were unoccupied.

Several subsequent papers supported this model on the basis of conductivity measurements (8), thermogravimetry (9) and X-ray Rietveld refinements (10). In the latter study, the structural model did not incorporate the planar features directly, but instead refined the cell size, strain, and site occupancy of the perovskite phase. At high substitution levels, new small peaks were observed in the powder X-ray diffraction pattern which were attributed to planar faulting or lamellar intergrowth.

While the evidence for the presence of additional oxygen in La-substituted $SrTiO_3$ is strong, the manner in which it is accommodated has thus far been investigated only by indirect methods. The present study therefore sought to determine the structure of these compounds directly using high-resolution electron microscopy (HREM). X-ray diffraction was also employed to ensure that the microscopic detail was consistent with the "average structure" obtained through diffraction from bulk samples.

EXPERIMENTAL

The raw materials used for synthesis were $SrCO_3$ (99%, BDH Chemicals Ltd.), TiO_2 (99.9 + %, Aldrich Chemical Co.), and La_2O_3 (99.9%, Ventron GMBH). Because of the strong tendency of La_2O_3 to form hydroxides when exposed to moist air, a stock of La_2TiO_5 was pre-

0022-4596/95 $6.00

pared and used as the La source for all subsequent experiments. Samples with compositions between $x = 0$ and $x = 1$ were prepared from mixtures of $SrCO_3$, La_2TiO_5, and TiO_2 by conventional solid-state synthesis, heating at 1350°C for 16 hr in air unless otherwise noted.

Phase composition was determined by X-ray powder diffraction (XRD) using a Philips goniometer and CuK_α radiation. For unit cell refinements, slower step scans were collected and peak positions were determined by fitting profiles to each peak with the Philips proprietary PC-APD software; these positions were used as input to a least-squares refinement program. Powder pattern calculations to assist with the assignment of indices were performed by the program POWD10 (11).

Samples for HREM were prepared by dispersing a suspension of the powder in acetone onto a holey carbon film supported by a copper grid. The JEOL 200CX microscope had been specially modified with a side entry stage and a high-resolution ($C_s = 0.41$) pole piece and was operated at 200 kV. Images were recorded at magnifications of ca. 450,000×, using current densities not exceeding 0.2 pA cm^{-2}. The precise magnification was established from calibration curves constructed from micrographs and electron diffraction patterns of $SrTiO_3$ taken over a range of objective lens currents. No evidence of structural alteration under electron irradiation was observed. Images simulated by the multislice method were used to confirm the proposed structure of the HREM images and were performed by the commercial CERIUS software. Elemental analysis using EDS could not be performed due to the considerable overlap between TiK and LaL X-ray emission lines.

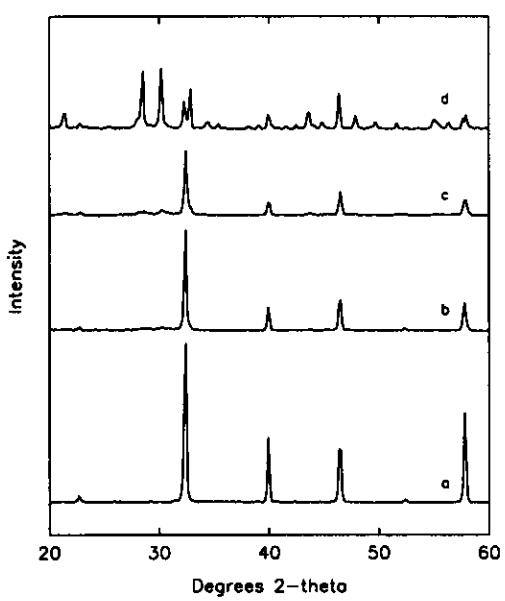

FIG. 1. Region of XRD patterns for representative samples of $Sr_{1-x}La_xTiO_{3+0.5x}$. Values of x are (a) 0; (b) 0.2; (c) 0.5; and (d) 0.8.

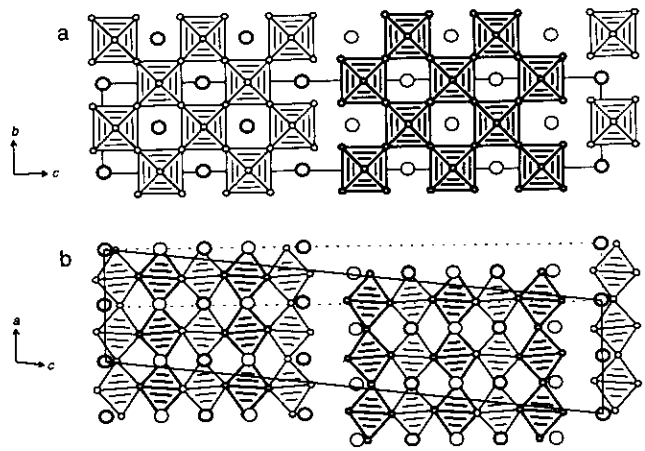

FIG. 2. Schematic structure of $La_5Ti_5O_{17}$ in (a) [100] and (b) [010] projections. Ti atoms lie at the centers of the octahedra, O atoms are small circles, and La atoms large circles. The heavy and light ruling indicates a difference in height along the viewing direction. Unit cells are outlined; in (b) the dashed cell shows the strong orthogonal subcell determined by cation positions only.

RESULTS

X-Ray Diffraction

A number of samples with compositions spanning the entire $Sr_{1-x}La_xTiO_{3+0.5x}$ substitution range were prepared and examined by XRD. Figure 1 shows a region of the XRD pattern for four representative samples. As the level of substitution was increased, the perovskite peaks became broader and less intense until new weak peaks could be discerned above the background for samples of composition $x = 0.4$–0.5. Upon further La substitution, the intensity of these peaks increased at the expense of the perovskite peaks so that only the peaks of the new phase were identifiable for the composition $x = 0.8$ (Fig. 1d). Although there was considerable overlap between the diffraction peaks of the new phase and those of $SrTiO_3$, the fact that the intensity ratios between these peaks did not change with further La substitution led us to believe that the perovskite phase was no longer present in significant concentrations at the $x = 0.8$ composition.

The XRD pattern of the $x = 0.8$ phase strongly resembled that of the reduced lanthanum titanate $La_5Ti_5O_{17}$ described recently by Williams *et al.* (12), suggesting that the two may be structurally analogous. The structure (Fig. 2) is related to that of $La_2Ti_2O_7$ (13) and consists of slabs of the perovskite structure bounded by planes which are parallel to a perovskite {110} plane. Adjacent slabs are displaced perpendicular to this plane, and are also displaced in the a direction by half an octahedron. The [010] projection of this structure drawn in Fig. 2b

shows how the cooperative tilting of the octahedra leads to monoclinic symmetry and a doubling of the *a* cell dimension. In $La_2Ti_2O_7$ the perovskite slabs are four octahedra wide, in $La_5Ti_5O_{17}$ they are five octahedra wide, and both compounds are members of a family of layered structures, with the general formula $A_nB_nO_{3n+2}$, formed in a variety of systems (14). The $x = 0.8$ compound ($SrLa_4Ti_5O_{17}$) and $La_5Ti_5O_{17}$ are $n = 5$ members of this family.

High-Resolution Electron Microscopy

HREM images of the $SrLa_4Ti_5O_{17}$ ($x = 0.8$) composition were taken in order to verify that this compound belonged to the family of $A_nB_nO_{3n+2}$ structures. Comparison of the experimental image taken in the [100] direction with a simulated image for $La_5Ti_5O_{17}$ (Fig. 3) confirmed that this assignment of the structure was justified. The agreement between the observed and calculated image is very good, although the canting of octahedra within the perovskite slabs observed by Williams *et al.* (12) for $La_5Ti_5O_{17}$ is less pronounced in the Sr-containing compound. This may be because the larger Sr^{2+} ion more closely matches the size of the appropriate site within the perovskite blocks.

Samples with lower levels of La substitution also displayed the same layered features in their HREM images. Figure 4 shows examples from samples with a composition corresponding to $x = 0.4$ in which clusters of $La_2Ti_2O_7$ type layers (Fig. 4a), as well as isolated layers (Fig. 4b), can be seen. In the images obtained in the present study, it was found that the layers appeared predominantly in clusters with a separation of approximately 30 Å.

Although extensive efforts were made to image similar features in samples with very low levels of La substitution, no suitable crystals could be found in the electron microscope. This was thought to be due to the difficulty

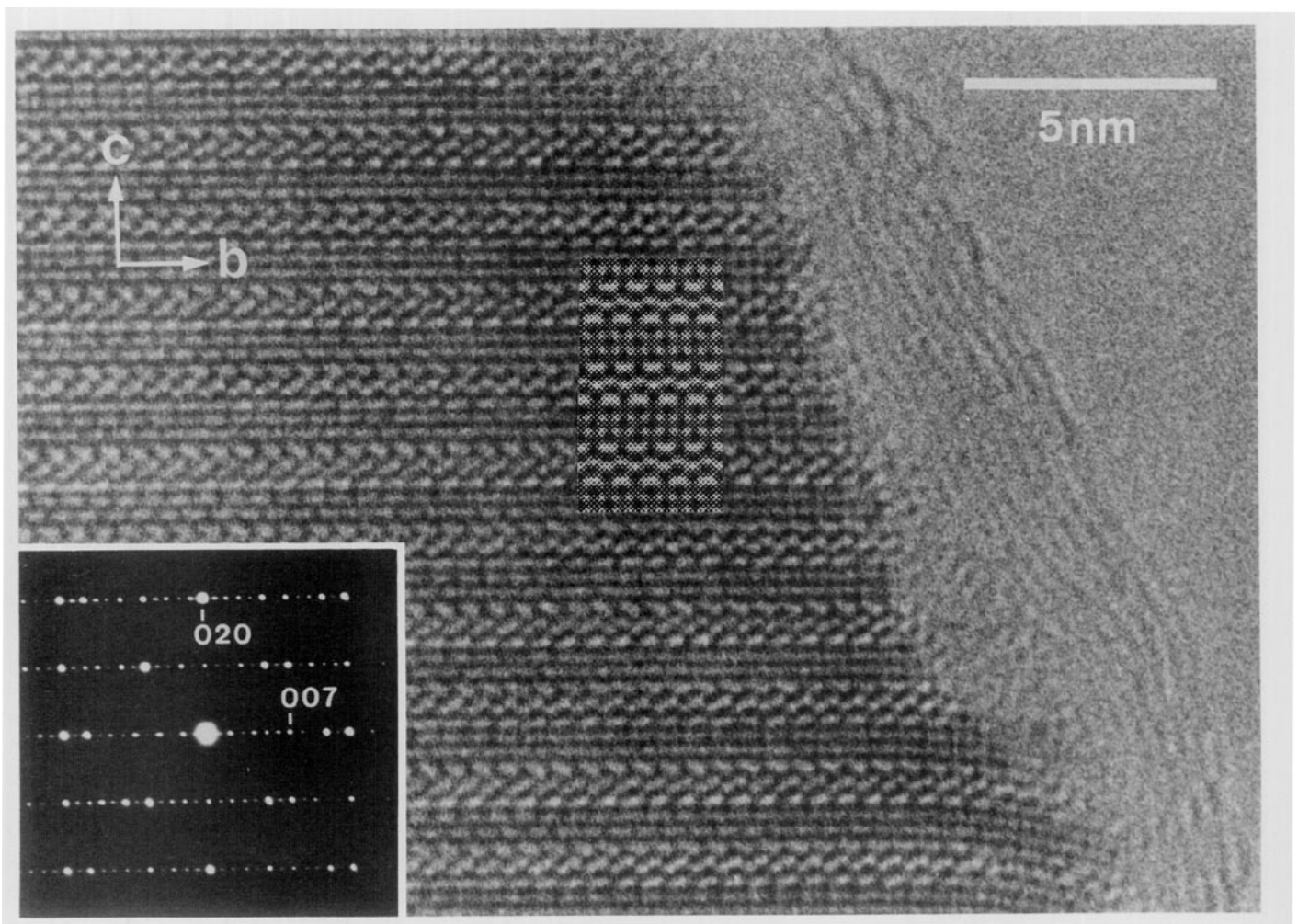

FIG. 3. HREM image of $SrLa_4Ti_5O_{17}$ taken in the [100] direction. The electron diffraction pattern and calculated image for $La_5Ti_5O_{17}$ (defocus −300 Å, thickness 23.6 Å) are inset.

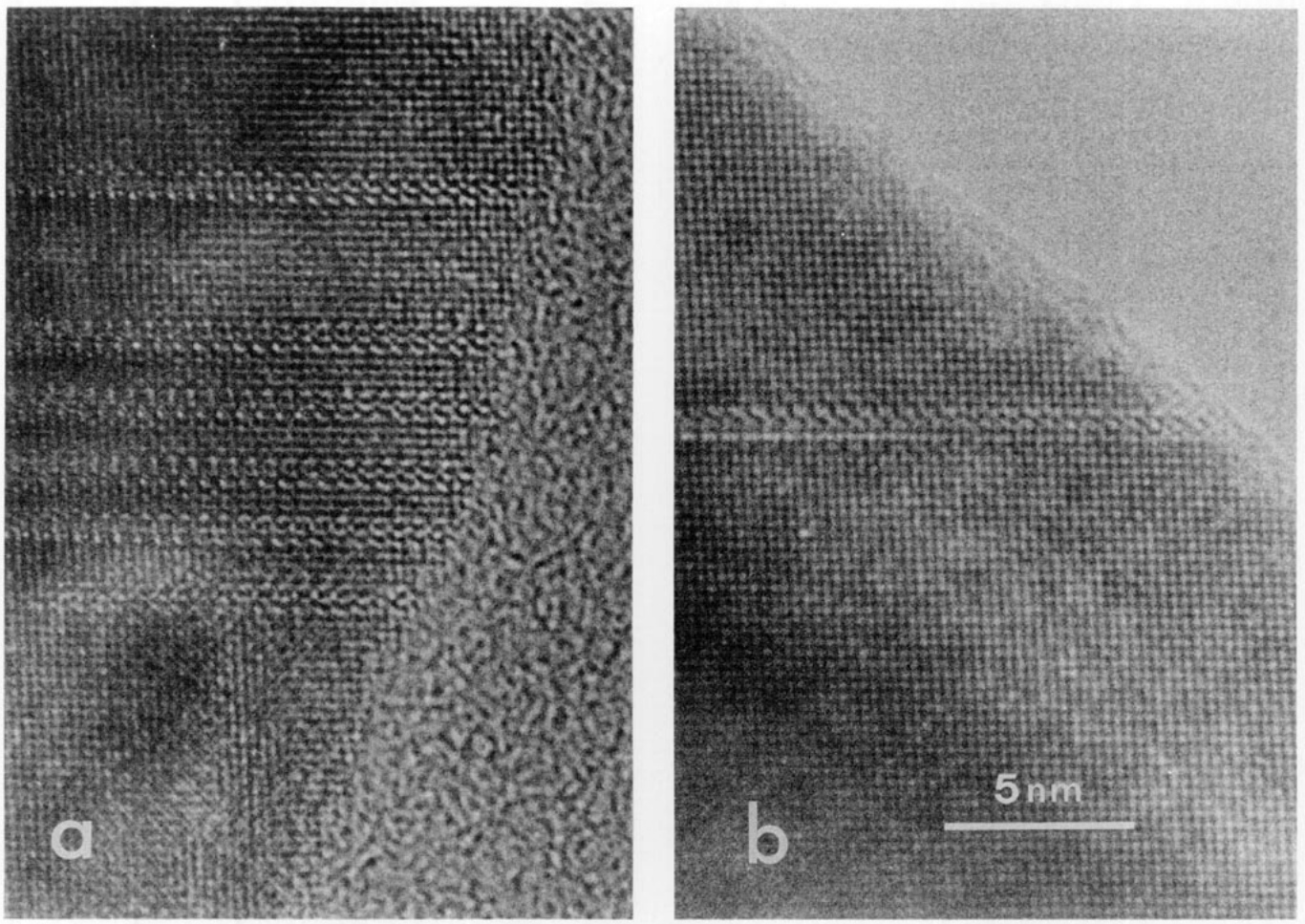

FIG. 4. HREM images from samples with an $x = 0.4$ composition. The layer structure can be identified by comparison with Fig. 3.

of finding suitable crystals lying in an appropriate orientation rather than to a lack of $La_2Ti_2O_7$ type layers in the samples. However, images were readily obtained which were consistent with the layer structure viewed perpendicular to the layer plane. The repeat distances in both the image and electron diffraction pattern shown in Fig. 5 correspond to the *a* and *b* dimensions (5.53 and 3.93 Å respectively) of $La_5Ti_5O_{17}$. In addition, the electron diffraction pattern showed weaker spots indicating a doubling of the *a* dimension, again comparable to the reported behavior of $La_5Ti_5O_{17}$ (12). The material appeared to have a preference for cleaving along planes parallel to the layer structure and the likelihood of locating suitably thin crystals with the layers parallel to the electron beam diminished with decreasing La substitution.

No evidence was found in HREM images for the presence of layers with structures similar to those found in $Sr_{n+1}Ti_nO_{3n+1}$ compounds. These compounds have tetragonal symmetry and could not account for the axial dimensions observed in Fig. 5.

DISCUSSION

Accommodation of Excess Oxygen

The formation of layers possessing the $La_2Ti_2O_7$ type structure provides a reasonable explanation of how additional oxygen is incorporated into the $SrTiO_3$ perovskite matrix when La^{3+} is substituted for Sr^{2+}. In layer structures of this type, the TiO_6 octahedra at the surfaces of the perovskite slabs corner-share oxygen atoms with only four other octahedra instead of the usual six, effectively inserting an additional plane of oxygen atoms at the planar boundary. This mechanism does not require lattice vacancies to explain the observed stoichiometries and operates over the whole range of substitution up to $La_2Ti_2O_7$ itself.

For compositions close to $SrTiO_3$ the occurrence of these oxygen-rich layers is relatively infrequent. For example, each layer in an $x = 0.2$ composition will be separated by, on the average, 20 octahedra of the perovskite

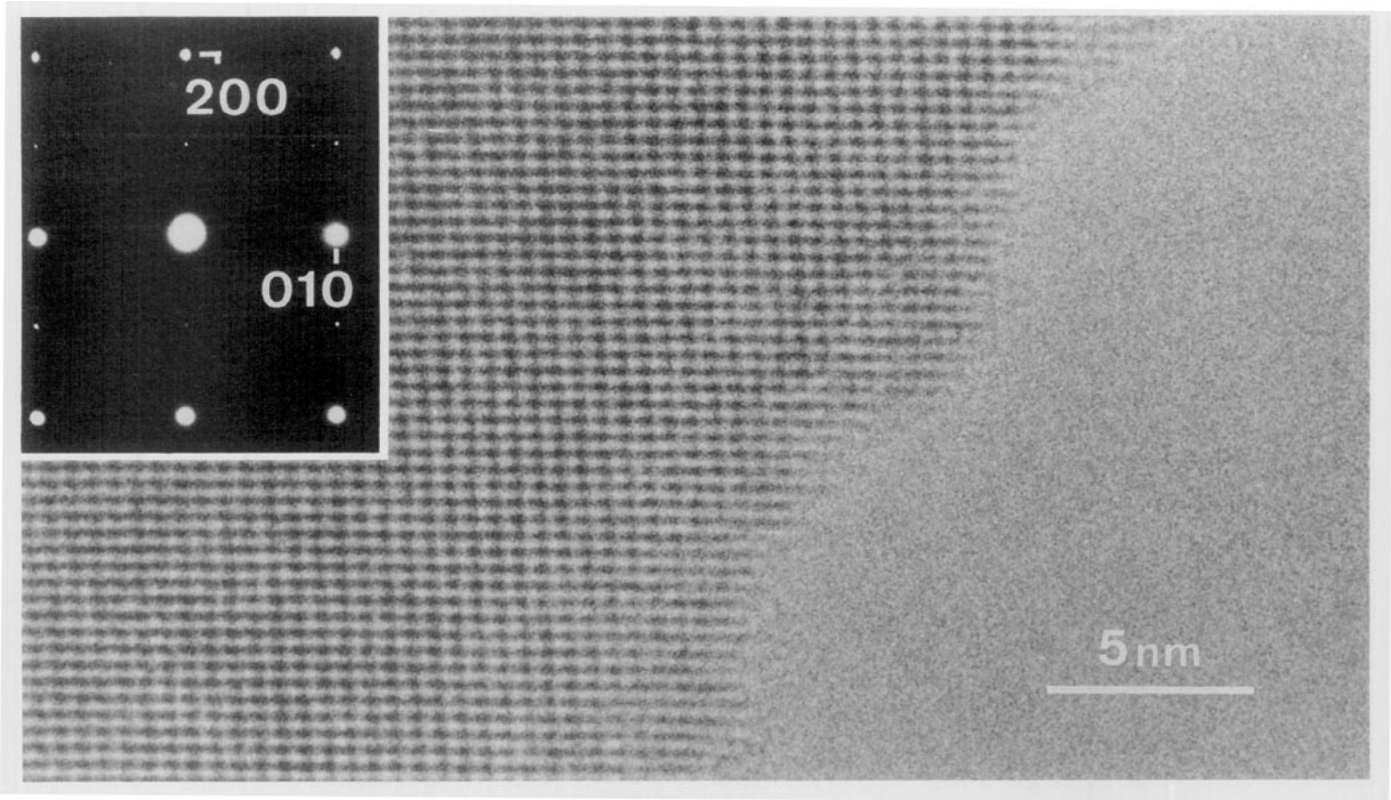

FIG. 5. HREM image and electron diffraction pattern from a specimen with a composition corresponding to $x = 0.2$. The diffraction pattern is indexed for the equivalent direction of the $SrLa_4Ti_5O_{17}$ cell.

structure. HREM has shown that the layers are not uniformly distributed and so large regions of perovskite remain. This accounts for the corresponding XRD patterns which show only perovskite peaks broadened by the strain and reduction in effective crystallite size produced by the incorporation of planar discontinuities. As substitution is increased, so too is the frequency of layers and they begin to form larger clusters with similar layer spacings, reflected in XRD traces with the emergence of new weak peaks. Only at very high levels of substitution do the layers order into recognizable new compounds.

The structural change occurring during the formation of these layers amounts to the insertion of a plane of oxygen atoms coupled with the relative displacement of the perovskite blocks on either side. The relative simplicity of this change is reflected in the readily reversible nature of the transformation between oxidized and reduced states of La-substituted $SrTiO_3$ (4). The structural scheme outlined in this study is also consistent with the evidence presented in previous studies of the $Sr_{1-x}La_xTiO_{3+0.5x}$ system which supported the model based on SrO layers and Sr vacancies. Both the conductivity measurements (8) and the thermogravimetric treatment (9) used to substantiate the SrO layer model conform equally well to the scheme proposed in the present study. Although Howard *et al.* (10) considered $Sr_3Ti_2O_7$ as the phase most likely to be responsible for the weak peaks observed in XRD traces from samples with high La contents, the XRD pattern of $La_5Ti_5O_{17}$ was not available at the time of these authors' study. In fact, this compound provides a better match to the XRD peaks.

Order–Disorder in the $Sr_{1-x}La_xTiO_{3+0.5x}$ System

A layered system such as this offers considerable scope for structural disorder, particularly in the stacking of the layers. Examples of disorder observed by HREM are shown in Fig. 6—random intergrowth of different layer spacings, tilt boundaries, and termination of the layer structure within a perovskite region. The last of these defects suggests a mechanism through which oxygen can be reversibly added to La-doped $SrTiO_3$, by the nucleation and growth of $La_2Ti_2O_7$ type layers within the perovskite matrix. The region near the end of such an incomplete layer must be considerably distorted, for not only are the perovskite regions on either side of the layer pushed apart owing to the extra oxygen atoms, they are also at different heights parallel to the viewing direction

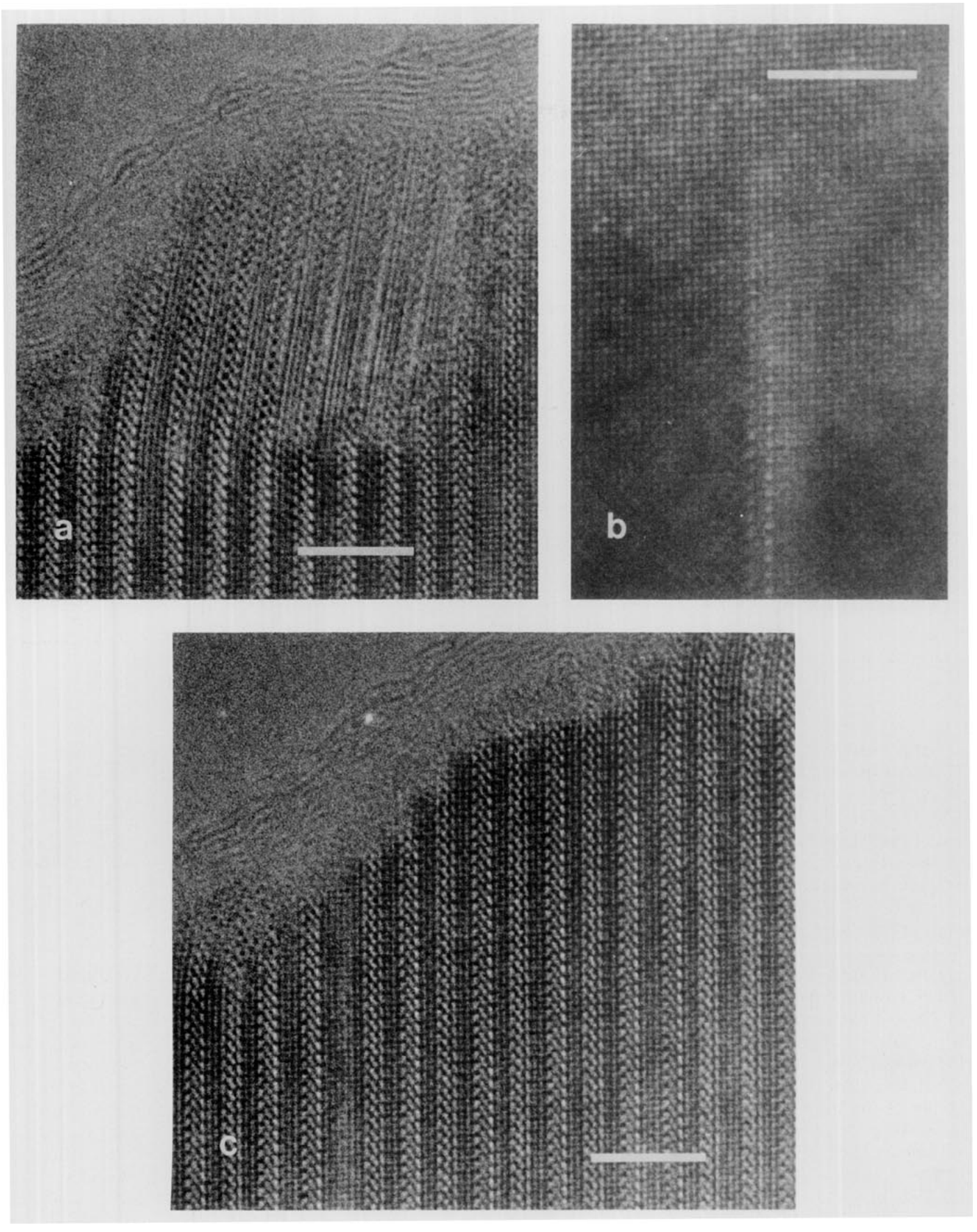

FIG. 6. Examples of layer disorder observed by HREM in samples of various composition: (a) tilt boundary; (b) termination of layer structure inside the crystal; and (c) irregular intergrowth of different layer spacings. The scale bars represent a distance of 5 nm.

of Fig. 6. Clearly neither of these displacements can persist beyond the end of the layer. Nevertheless, several occurrences of this type of defect were found by using HREM, particularly in samples with low La contents. Williams *et al.* (15) have observed the same type of defect in structural analogues in the Sr–La–Nb–O system, and have shown that reduction within the electron microscope results in the layer structure retreating from the crystal surface.

By contrast, specimens with well-ordered layer spacings were far less frequent and only two ordered compounds could be prepared. The first of these, $SrLa_4Ti_5O_{17}$, has already been referred to in the XRD results, and is the $n = 5$ member of a series $Sr_{n-4}La_4Ti_nO_{3n+2}$. The monoclinic unit cell was refined from the XRD peak positions to give the dimensions $a = 7.812(4)$ Å, $b = 5.529(1)$ Å, $c = 31.51(1)$ Å, $\beta = 97.13(3)°$. Although the XRD peaks could also be indexed on an orthorhombic cell with half the a dimension, [010] electron diffraction patterns confirmed the monoclinic symmetry, which almost certainly arises from the small shifts in the oxygen sublattice depicted in Fig. 2. The XRD pattern is not tabulated here because of its similarity to $La_5Ti_5O_{17}$.

The other ordered compound prepared was the $n = 4.5$ member of the same series, identified by HREM and XRD as an ordered intergrowth of $La_2Ti_2O_7$ and Sr $La_4Ti_5O_{17}$. The HREM image (Fig. 7) displayed a strict alternation of $n = 4$ and $n = 5$ layers and the electron diffraction pattern shown inset indicated a long axis with the expected spacing of ~57 Å. The simulated HREM image also shown in this figure was calculated from a set of idealized atomic coordinates for the intergrowth structure generated on the basis of interatomic distances found in $La_5Ti_5O_{17}$.

To confirm that this microscopic observation was indicative of the bulk structure, an XRD pattern was calculated from the idealized structure and used to assign Miller indices to the observed peaks. All the peaks in the XRD pattern could be ascribed to an orthorhombic cell with the refined dimensions $a = 7.810(2)$ Å, $b = 5.533(2)$

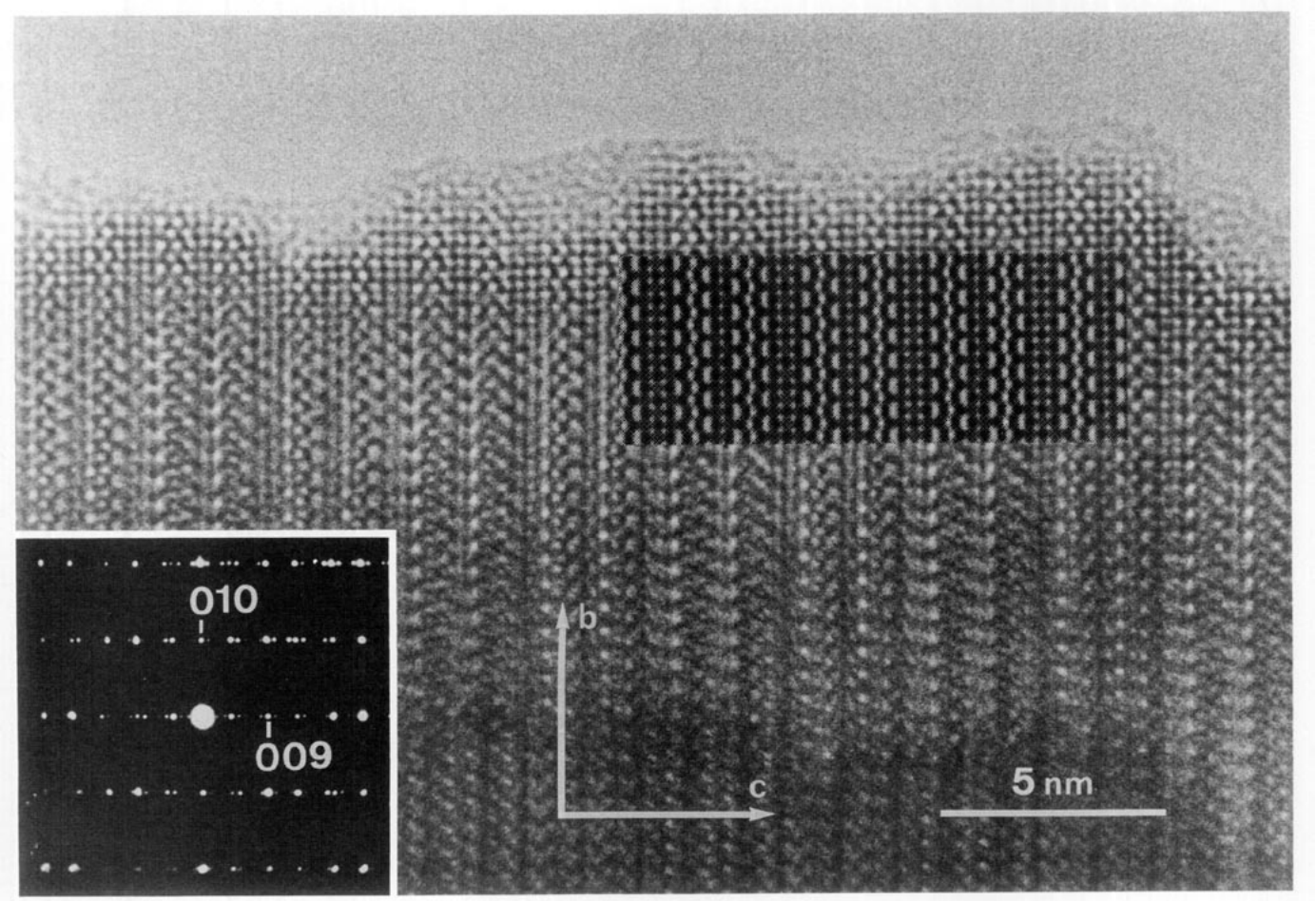

FIG. 7. Ordered intergrowth of $La_2Ti_2O_7$ and $SrLa_4Ti_5O_{17}$ layers with corresponding electron diffraction pattern and simulated image (defocus −315 Å, thickness 23.4 Å) inset.

TABLE 1
Calculated and Observed X-Ray Diffraction Pattern for $SrLa_8Ti_9O_{31}$ (CuK_α radiation)

h	k	l	d_{calc}	d_{obs}	I_{calc}	I_{obs}
0	1	9	4.167	4.153	64	40
1	0	2	3.869	3.861	16	14
0	1	18	3.437	3.438	4	3
0	0	18	3.167	3.161	61	70
1	1	3	3.146	3.124	61	70
1	1	7	2.971	2.975	100	78
0	1	17	2.868	2.870	13	6
0	2	0	2.767	2.762	51	58
1	1	11	2.717	2.714	95	100
1	0	16	2.632	2.630	24	13
0	0	22	2.591	2.595	2	5
1	0	20	2.302	2.300	22	9
1	2	2	2.250	2.249	43	40
1	1	19	2.186	2.190	6	3
0	2	18	2.084	2.082	71	15
1	1	21	2.068	2.069	11	26
2	0	0	1.9525	1.9518	45	64
0	2	22	1.8913	1.8919	9	18
1	1	25	1.8553	1.8536	13	6
2	1	9	1.7681	1.7675	12	15
1	1	29	1.6737	1.6734	13	8
2	0	18	1.6621	1.6629	17	18
1	3	7	1.6338	1.6337	15	9
2	2	0	1.5952	1.5950	18	29
1	3	11	1.5875	1.5874	17	27
1	1	33	1.5193	1.5203	3	7
2	2	18	1.4247	1.4249	33	20
2	2	22	1.3585	1.3593	4	9
3	1	7	1.2520	1.2524	6	8
3	1	11	1.2308	1.2316	7	8

Å, c = 57.01(2) Å. Note that it is not necessary to consider a monoclinic cell for this compound because the oxygen sublattice reverts to its original configuration after the layer repeat of two layers each of the n = 4 and n = 5 members. The observed and calculated XRD patterns are compared in Table 1 and, although the agreement between observed and calculated intensities is not perfect, they are sufficiently close to engender confidence in the assignment of the indices. Better agreement could be obtained by refining the idealized model; however, the intention of the present work was only to illustrate the overall structure.

Nanot *et al.* (16) have reported the analogous n = 4.5, 5, and 6 compounds in the Ca–La–Ti–O system. However, the n = 6 member of the Sr-containing series could not be synthesized, despite prolonged reactions at temperatures up to 1450°C. After a single overnight heating of this composition at 1350°C, the XRD pattern showed primarily broadened perovskite peaks with minor peaks attributed to $SrLa_4Ti_5O_{17}$. With further heating, the perovskite peaks sharpened and the $SrLa_4Ti_5O_{17}$ peaks grew to finally yield a steady state mixture of the two oxides, which was assumed to be the equilibrium state. This slow ordering process may also account for the early conflict over whether La has appreciable solubility in $SrTiO_3$. The very high synthesis temperature (1500°C) employed by Tofield and Scott (1) led to the ordering of a second phase and to their conclusion that $SrTiO_3$ could accept only limited substitution. Balachandran and Eror (3), on the other hand, used more modest reaction conditions (1350°C) and therefore observed the disordered "solid solution" indicated by the presence of only perovskite peaks in the XRD pattern.

CONCLUSIONS

The substitution of La for Sr in $SrTiO_3$, when heated in oxidizing atmospheres, results in the formation of oxygen-rich layers within the perovskite matrix. High-resolution electron microscopy shows that the structure of these layers is the same as for those found in $La_2Ti_2O_7$. The situation is very similar to that which exists in the

conventional "Ruddlesden–Popper" phases such as $Sr_{n+1}Ti_nO_{3n+1}$, except that in the $Sr_{1-x}La_xTiO_{3+0.5x}$ case the planes of oxygen atoms are parallel to the {110} planes of the parent perovskite, rather than to the {100} planes in the former. One other important difference arises from the fact that the planes of oxygen atoms in both orientations can be grouped into two types, one containing more atoms than the other. In the Ruddlesden–Popper phases the extra plane inserted has a lower density of oxygen atoms, whereas in $Sr_{1-x}La_xTiO_{3+0.5x}$ the most dense plane is inserted. This, in turn, is to be expected when cations of greater valency are being substituted into the perovskite structure.

The compounds produced by this substitution are better described as a structural solid solution of $La_2Ti_2O_7$ type layers in $SrTiO_3$ rather than as the customary atomic solid solution. This solution occurs across the entire $Sr_{1-x}La_xTiO_{3+0.5x}$ compositional range, although at higher levels of substitution ($x \geq 0.8$) the layers order into new compounds detectable by diffraction methods. These compounds are represented by the general formula $Sr_{n-4}La_4Ti_nO_{3n+2}$ and the $n = 4.5$ and $n = 5$ members have been prepared in the present investigation. Less-substituted materials contain a lower concentration of the layers distributed throughout the perovskite host; usually more are found in groups than as isolated features. When they are distributed randomly, X-ray diffraction patterns show only a broadened perovskite signal, but if specimens are heated for prolonged times, the layers may order in domains to give a two-phase mixture.

ACKNOWLEDGMENT

MEB gratefully acknowledges the generous financial support provided by a study award from the New Zealand Institute for Industrial Research and Development.

REFERENCES

1. B. C. Tofield and W. R. Scott, *J. Solid State Chem.* **10,** 183 (1974).
2. J. Bouwma, K. J. DeVries, and A. J. Burggraaf, *Phys. Status Solidi A* **35,** 281 (1976).
3. U. Balachandran and N. G. Eror, *J. Am. Ceram. Soc.* **64,** C75 (1981).
4. N. G. Eror and U. Balachandran, *J. Solid State Chem.* **40,** 85 (1981).
5. S. N. Ruddlesden and P. Popper, *Acta Crystallogr.* **10,** 538 (1957).
6. S. N. Ruddlesden and P. Popper, *Acta Crystallogr.* **11,** 54 (1958).
7. R. J. D. Tilley, *J. Solid State Chem.* **21,** 293 (1977).
8. U. Balachandran and N. G. Eror, *J. Electrochem. Soc.* **129,** 1021 (1982).
9. B. F. Flandermeyer, A. K. Agaral, H. U. Anderson, and M. M. Nasrallah, *J. Mater. Sci.* **19,** 2593 (1984).
10. S. A. Howard, J. K. Lau, and H. U. Anderson, *J. Appl. Phys.* **65,** 1492 (1989).
11. D. K. Smith, M. C. Nichols, and M. E. Zolensky, "A Fortran-IV Program for Calculating X-ray Diffraction Patterns—Version 10," Pennsylvania State University, Department of Geosciences, University Park, PA, 1983.
12. T. Williams, H. Schmalle, A. Reller, F. Lichtenberg, D. Widmer, and G. Bednorz, *J. Solid State Chem.* **93,** 534 (1991).
13. M. Gasperin, *Acta Crystallogr. Sect. B: Struct. Sci.* **31,** 2129 (1975).
14. R. J. D. Tilley, *Chem. Phys. Solids Their Surf.* **8,** 121 (1980).
15. T. Williams, F. Lichtenberg, D. Widmer, J. G. Bednorz, and A. Reller, *J. Solid State Chem.* **103,** 375 (1993).
16. M. Nanot, F. Queyroux, and J.-C. Gilles, *C.R. Acad. Sci. Paris C* **277,** 505 (1973).